4

Transmission, Reflection and Thermal Radiation of a Magneto-Optical Fabry-Perot Resonator in Magnetic Field: Investigations and Applications

Anatoliy Liptuga, Vasyl Morozhenko and Victor Pipa
V. Lashkaryov Institute of Semiconductor Physics, Kyiv, Ukraine

1. Introduction

Recent years, considerable attention is paid to the study of the optical properties of plane-parallel mono- and multilayer resonator structures based on dielectric, semiconductor and metallic media. Interference effects in such structures set conditions for their selective properties with respect to wavelength, direction of propagation and polarization of light. These effects result in modification of the spectral and angular characteristics of the intensity of transmitted, reflected, and self-emitted (e.g., thermal emission) light. Application of magnetic materials as components of the structures has opened up quite a number of possibilities, which have both scientific and applied importance. First, the magneto-optical methods are very effective for investigation of the parameters of materials and characteristic properties of the structures. Second, the synthesis of new magnetic materials, selection of their dimensions and location will make possible to create a new generation of optical devices controlled by a magnetic field (H): displays and data-transmission systems, sources and sensors of light, magneto-optical modulators and shutters etc. In this case, it concerns not only visible but also infrared (IR) light.

To use the multiple reflections for enhancement of the magneto-optical rotation was proposed by Faraday itself. As a result of the fact that the direction of the rotation does not depend on direction of a magnetic field, he achieved an increase of the light path length in the sample by silvering its surfaces. In those years, samples were sufficiently thick and less than perfect and they did not take into account the interference effects.

The first one who has denoted on a necessity to consider interference effects in the measurements of the Faraday rotation angle was Voigt (Voigt, 1904), but only in the second half of the 20th century with the appearance of the plane-parallel samples with sufficient quality, the study of peculiarities of the Faraday effect in the presence of interference has found its experimental and theoretical advancement. In one of the first papers (Rosenberg et al., 1964) it was shown that the Faraday rotation can be resonantly enhanced by a Fabry-Perot resonator. The importance of considering the effects of internal multiple reflections in the measurements of the Faraday rotation angle was noted by the authors (Piller 1966; Rheinhlander et al, 1975; Stramska et al. 1968; Srivastava et al, 1975; Vorobev et al, 1972).

In the subsequent studies (Jacob et al, 1995; Ling, 1994; Wallenhorst et al 1995) attention was paid to the theoretical and experimental studies of not only the Faraday rotation angle, but also to the studies of a state of light polarization and transmission function of the simple resonance objects such as Fabry-Perot resonators. Based on the obtained results authors have concluded that the application of the Fabry-Perot resonator is an effective method for a measuring of the Faraday rotation, especially in the inefficient media. It was also mentioned that this effect can be used in the spectroscopic devices.

As an impact to active study of composite resonant magneto-optical structures it was the paper (Inoue & Fujii, 1997), in which the magneto-optical properties of the Bi:YIG films with random multilayer structures were researched. The authors have found a large enhancement in Faraday and Kerr effects in the structures. In the some subsequent papers such multilayer structures were named the magnetophotonic crystals (MPCs). Detailed review of these objects, their peculiarities and applications is presented in (Inoue et al. 2008).

Recently, the Faraday rotation was investigated in different types of structures including 2D and 3D MPCs (Dokukin et al. 2009; Fujikawa et al. 2009) and optical Tam structures (Goto et al., 2009a, 2009b). Moreover, the studies were done not only for the visible and near infrared light, but also in the far-infrared range (Zhu et al. 2011).

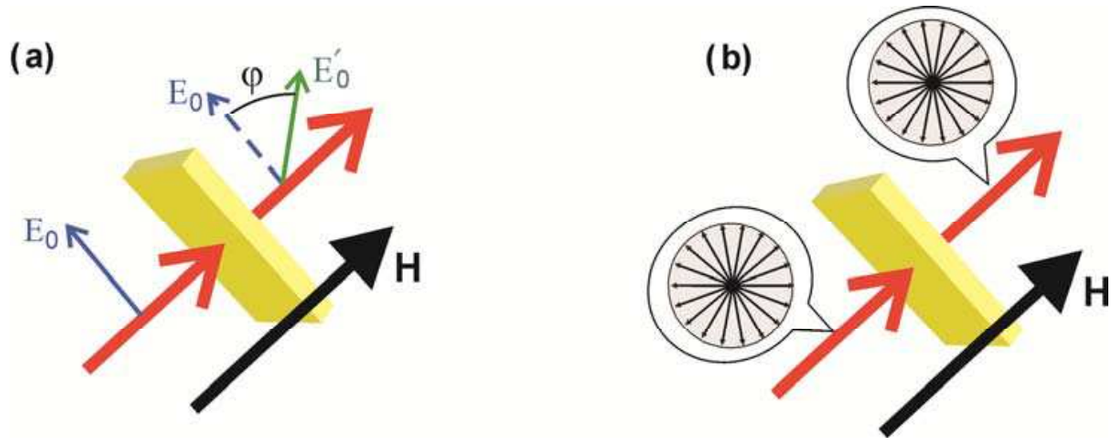

Fig. 1. (a) Demonstration of the Faraday rotation of linearly polarized light. $\mathbf{E_0}$ is a vector of electric field of the incident wave; $\mathbf{E'_0}$ is a vector of electric field of the transmitted wave, φ is the Faraday rotation angle.
(b) Demonstration of the Faraday rotation using unpolarized light. Balloons show the azimuth distribution of the linearly polarized components.

The investigations (Kollyukh et al., 2005; Morozhenko & Kollyukh, 2009) have shown that the influence of a magnetic field appears not only with respect to external linearly polarized light, but also with respect to their own thermal radiation (TR) of structure. This puts a question: does the Faraday rotation exist in unpolarized light? By definition, the Faraday effect is a rotation of the plane of polarization in a parallel to direction of propagation magnetic field, as it is shown in Fig.1a. Based on this, the obvious answer is no, because in the absence of the selected plane of polarization the rotation can not be fixed. This is clearly seen in Fig.1b. For this reason all studies of magneto-optical rotation are carried out with the linearly polarized light.

In this paper, based on the example of a magneto-optical Fabry-Perot resonator (MOR), it is shown that the uniqueness of the resonant magneto-optical structures is also that they are applicable for an unpolarized light. A change of their reflective and transmitting characteristics in a magnetic field using an unpolarized light is so effective as polarized.

The authors paid attention to the influence of a magnetic field to the angular and spectral characteristics of MOR in the middle-wave and long-wave IR, and the results of theoretical and experimental studies of thermal radiation of MOR are also presented and discussed.

On base of the obtained results it is described a number of possible applications of the effect. It is shown that this effect opens up the wide possibilities for developing both new controllable magneto-optical devices and methods of determination of the structure parameters.

2. Model and theory

Let us consider a magneto-optical Fabry-Perot resonator that consists of two non-absorbing mirrors with the reflection coefficients ρ_1, ρ_2 and a magneto-optical medium inside. The mirrors are spaced by a distance d. The medium is characterized by an isotropic at $H = 0$ complex refractive index $N = n + i\chi$ ($\chi << n$). An external magnetic field is perpendicular to the surface xy of the resonator.

The unpolarized light with wavelength λ and intensity I_0 falls on MOR at angle θ_1 (see Fig.2). Since the incident light is unpolarized, it contains equal quantities of the linearly polarized components with any planes of polarization. Propagating in the resonator the wave refracts and reflects back in a volume and splits into the series of coherent among themselves secondary waves j_ξ ($\xi = 0,1,2...$). Their coherence is determined by a coherence of their corresponding linearly polarized components. When the light is crossing the MOR, the planes of polarization of the linearly polarized components rotate. It is shown in the balloons of Fig.2.

For calculations of the light propagation with the Faraday rotation the matrix method of multi-beam summation (Morozhenko & Kollyukh, 2009) is used. A matrix-vector of electric field of an arbitrary linearly polarized component (see Fig.2) of the incident wave is (Yariv & Yen, 1984):

$$\mathbf{E_0} = E_0 \cdot \begin{bmatrix} \cos(\beta) \\ \sin(\beta) \end{bmatrix}, \tag{1}$$

where β is an azimuth of the component. Time dependence of $\mathbf{E}_0$ is omitted. A propagation of the linearly polarized components in the MOR is described by following matrices:

$$\mathbf{R_1} = \begin{bmatrix} r_1^{(s)} & 0 \\ 0 & -r_1^{(p)} \end{bmatrix}, \ \mathbf{R_2} = \begin{bmatrix} r_2^{(s)} & 0 \\ 0 & -r_2^{(p)} \end{bmatrix}, \ \mathbf{M_1} = \begin{bmatrix} t_1^{(s)} & 0 \\ 0 & t_1^{(p)} \end{bmatrix},$$

$$\mathbf{M_2} = \begin{bmatrix} t_2^{(s)} & 0 \\ 0 & t_2^{(p)} \end{bmatrix}, \ \mathbf{F} = \begin{bmatrix} \cos(\varphi) & \sin(\varphi) \\ -\sin(\varphi) & \cos(\varphi) \end{bmatrix} \mathrm{e}^{ik_z d}, \tag{2}$$

where $r_{1,2}^{(s),(p)}$ and $t_{1,2}^{(s),(p)}$ are the reflection and transmission amplitudes respectively for s- and p-polarizations, $k_z = (2\pi / \lambda)\sqrt{N^2 - \sin^2(\theta_1)}$, φ is a single-trip Faraday rotation angle.

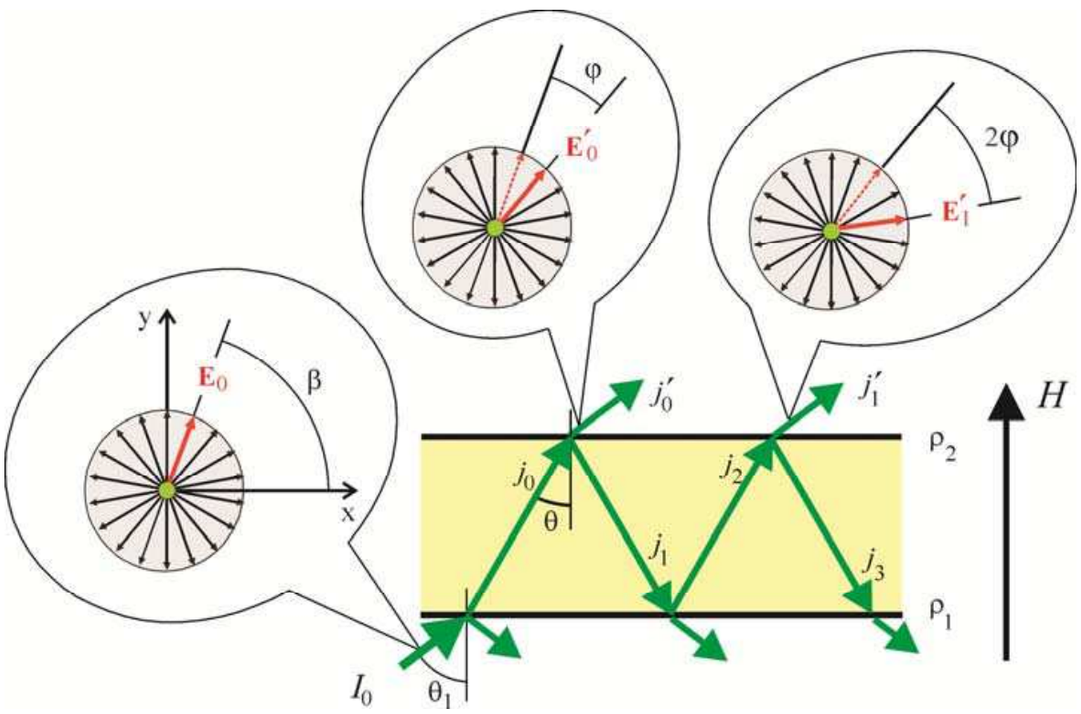

Fig. 2. Propagation of natural light in a magneto-optical Fabry-Perot resonator. Balloons show the azimuth distribution of the linearly polarized components. They are shown as at normal incidence for visualization and convenience.

The matrices $\mathbf{R_{1,2}}$ and $\mathbf{M_{1,2}}$ describe reflection and refraction respectively, $\mathbf{F}$ is a matrix of passage with the Faraday rotation.

The transmitted secondary waves are:

$$\mathbf{E}'_{\xi} = \mathbf{M_2}\left(\mathbf{FR_1FR_2}\right)^{\xi}\mathbf{FM_1E_0}\,. \tag{3}$$

The sum of the waves $\mathbf{E}'_{\xi}$ is the sum of matrix series

$$\mathbf{E}' = \mathbf{M_2}\left(\sum_{\xi=0}^{\infty}(\mathbf{FR_1FR_2})^{\xi}\right)\mathbf{FM_1E_0}\,. \tag{4}$$

It is easy to make sure to certain that for eigenvalue L of the matrix $\mathbf{FR_1FR_2}$ a condition $|L|<1$ is always true. Hence the sum in Eq. (4) can be replaced with the expression (Lancaster & Tismenetsky, 1985):

$$\mathbf{E}' = \mathbf{M_2}\left(\mathbf{I} - \mathbf{FR_1FR_2}\right)^{-1}\mathbf{FM_1E_0}\,, \tag{5}$$

where $\mathbf{I}$ is the unity matrix. This summarized wave is a component of a total summarized wave $j' = \sum j'_{\xi}$. Since the separate components are not coherent, to determine the total transmission T it is necessary to sum up the intensities of all transmitted components and divide it into I_0:

$$T = \frac{1}{2}\sum_{i,j}\left|u_{ij}\right|^2, \tag{6}$$

where u_{ij} are the elements of a matrix $\mathbf{M_2}\left(\mathbf{I}-\mathbf{FR_1FR_2}\right)^{-1}\mathbf{FM_1}$.

By doing the foregoing operations, it is possible to obtain an equations for reflection R:

$$R = \frac{1}{2}\sum_{i,j}\left|w_{ij}\right|^2 . \tag{7}$$

Here w_{ij} are the elements of a matrix $\left(\mathbf{M_1}\left(\mathbf{I}-\mathbf{FR_2FR_1}\right)^{-1}\mathbf{FR_2FM_1}+\mathbf{R_1}\right)$.

In case of thermal radiation (TR), the light is not external and radiated by a volume. The intensity of a "primary" wave, radiated at angle θ in a small solid angle $d\Omega$ and reached a boundary is

$$J_0 = (1-\eta)n^2 W\cos(\theta)d\Omega, \tag{8}$$

where W is the Planck function, $\eta = \exp(-\alpha d/\cos(\theta))$, $\alpha = 4\pi\chi/\lambda$ is an absorption coefficient. Since n and α are isotropic, this wave is unpolarized.

The intensity of TR that the MOR radiates from the mirror ρ_1 at angle θ_1 ($\sin(\theta_1) = n\cdot\sin(\theta)$) in a solid angle $d\Omega_1 = n^2 d\Omega\cos(\theta)/\cos(\theta_1)$ is

$$I_{TR} = \frac{1}{2}\sum_{i,j}\left(\left|q_{ij}\right|^2+\left|g_{ij}\right|^2\right)(1-\eta)W\cos(\theta_1)d\Omega_1, \tag{9}$$

where q_{ij} and g_{ij} are the elements of the matrix $\mathbf{M_1}\left(\mathbf{I}-\mathbf{FR_2FR_1}\right)^{-1}$ and $\mathbf{M_1}\left(\mathbf{I}-\mathbf{FR_2FR_1}\right)^{-1}\mathbf{FR_2}$ respectively.

In Equations (6), (7) and (9) the matrix elements "$i1$" describe the peculiarities of s-polarized part of light, and the elements "$i2$" describe the peculiarities of p-polarized one.

Equation (9) is the Kirchhoft's law for a magneto-optical Fabry-Perot resonator in a magnetic field. The factors to the left of the Planck function are an emissivity (A) of the resonator. The emissivity describes all TR features that are related to the dielectric and geometric properties of a heated object. For this reason to analyze the peculiarities of A sometimes is more convenient, than intensity of TR.

3. Results and discussions

3.1 Theoretical results

The calculations were carried out for the resonator with the reflection coefficients of the mirrors $\rho_1 = \rho_2 = 0.6$. Modeling magneto-optical medium has a complex refractive index $N = 3 + i\cdot 7.1\cdot 10^{-3}$ and thickness $d = 50$ μ m.

Fig.3 shows the theoretical dependence of the angular distribution of the MOR transmission (a) and reflection (b) on the single-trip Faraday rotation angle for unpolarized light. It is seen, at $H = 0$ the angular distributions of transmission and reflection have a lobe-like character and correspond to a number of the interference maxima (lobes) and minima with the high contrast.

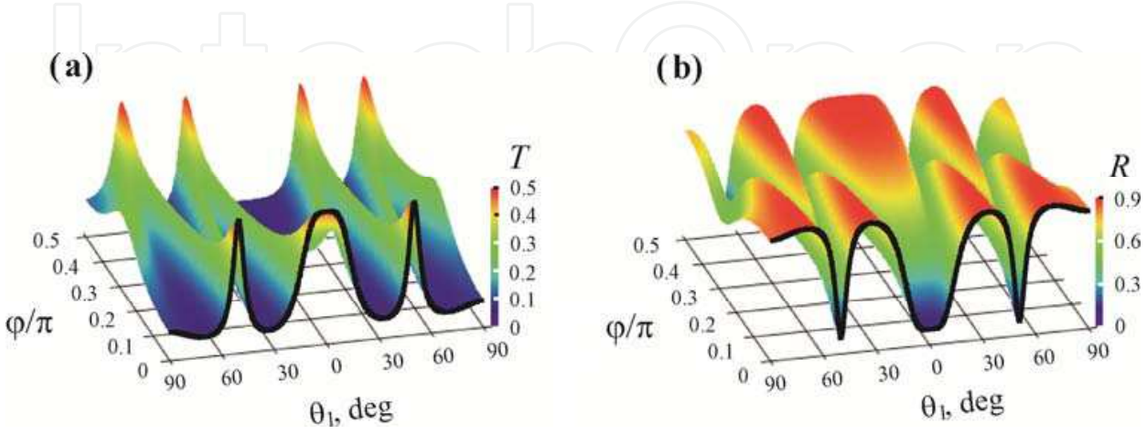

Fig .3. (a) Theoretical dependence of the angular distribution of the MOR transmission on magnetic field. Incident light is unpolarized. $\lambda = 10$ μ m.
(b) Theoretical dependence of the angular distribution of the MOR reflection on magnetic field. Incident light is unpolarized. $\lambda = 10$ μ m.

In the magnetic field the lobes of transmission split into two secondary lobes, which diverge and decrease in amplitude as the field is increasing. For $\varphi = \pi / 4$, the contrast of the angular distribution reaches a minimal value.

With a further increasing field the secondary lobes begin to merge pairwise with the neighboring one and at $\varphi = \pi / 2$ the angular distribution of the transmission takes a pronounced lobe-like character again. However, there is an inversion of the interference extrema: positions of the lobes correspond to the minima at $H = 0$.

Behavior of the angular distribution of reflection in the magnetic field differs from that discussed above for transmission distribution. In this case the interference minima split. Maxima lobes appear in their place with intensity increasing with increasing of the magnetic field.

When $\varphi = \pi / 4$, the amplitudes of the original lobes (at $H = 0$) are almost equal to the amplitude of the appearing ones and the angular distribution of R become practically homogeneous.

At $\varphi = \pi / 2$ the angular distribution of R has a lobe-like character again, but with the inversion of the resonance extrema.

The cause of the changes of the angular distributions of T and R is a change of the conditions of the multibeam interference in the magnetic field. The magnetic field

redistributes the polarization planes of the waves of light inside the resonator. As a result, the interference of the transmitted and reflected waves can be suppressed or phase shifted by a phase difference of π .

In Fig.4 the directional diagrams of the resonator's TR are shown for $\lambda = 10 \quad \mu$ m at different values of φ . With $\varphi = 0$ the directional diagram has a muti-peaked antenna pattern with a narrow central main lobe and an axially symmetric radially diverging secondary (conical) lobe. The intensities of the lobes and their ratio are dependent on the resonator parameters such as the coefficients of reflection $\rho_{1,2}$, absorption of the magneto-optical medium (Guga et al. 2004), MOR temperature and wavelength. In order to eliminate the last two parameters, the directional diagrams are shown in arbitrary units.

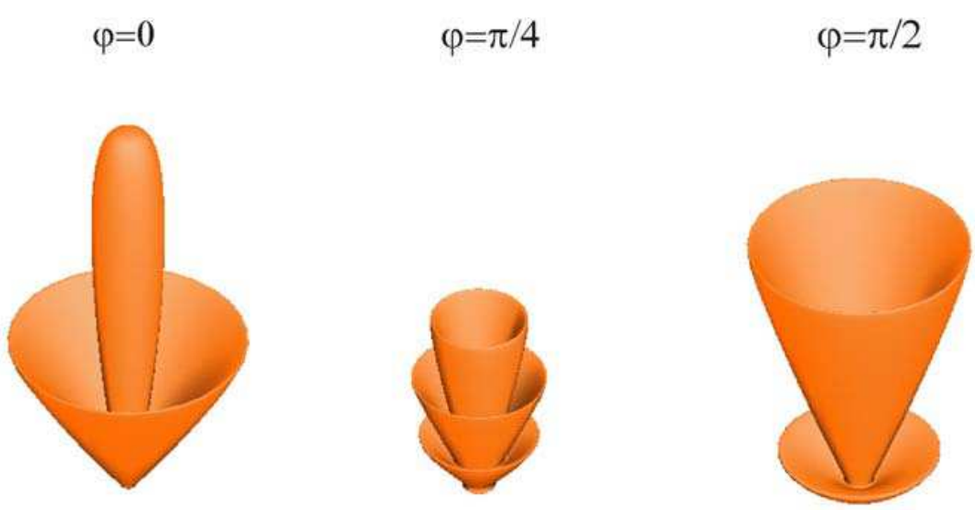

Fig. 4. Modification of TR directional diagram for $\lambda = 10 \quad \mu$ m at different values of φ .

In the magnetic field, when $\varphi = \pi / 4$, the directional diagram supports a greater number of relatively weak minor lobes, making the radiation more uniform, making it more like TR from a nonresonant object.

When the Faraday rotation reaches a value $\varphi = \pi / 2$ the directional diagram takes on a clear multi-lobed structure again, but with no axially directed maximum radiation. The central lobe is missing and the axial radiation is minimum. Only flared minor lobes are present. Therefore, the magnetic field determines the directional diagram of TR and this property of resonator can be used to generate controlled sources of infrared radiation.

Fig. 5 presents the calculated fringes of constant inclination of the transmitted light when MOR is illuminated by an unpolarized polychromatic $\lambda = 9.668 - 10 \quad \mu$ m source. The calculations are limited to the first interference order. As it is seen, at $\varphi = 0$ the fringes have a form of contrasting rings, painted in accordance with the wavelength of the interference lobe (the scale of wavelengths is shown on the right).

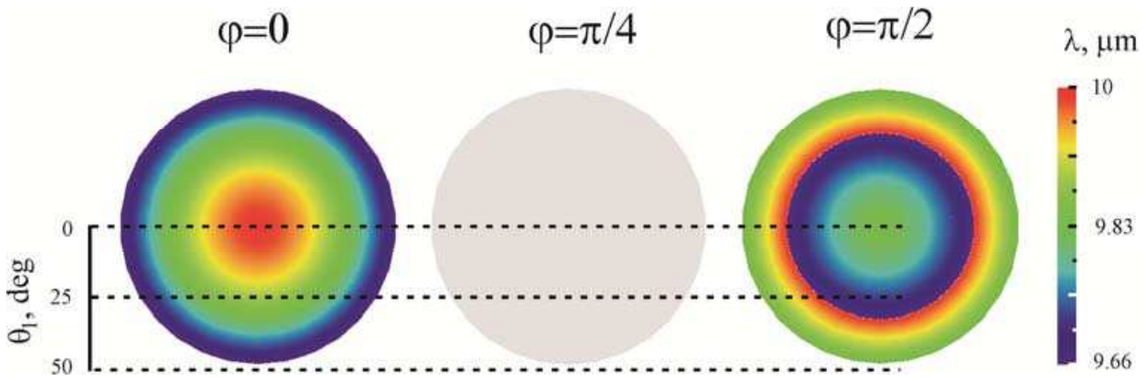

Fig. 5. Fringes of constant inclination of the MOR. The incident light is unpolarized. $\lambda = 9.668 - 10$ μ m. The wavelength scale is shown on the right.

When $\varphi = \pi / 4$ the angular dispersion of the resonator disappears. The transmitted light does not have the selected wavelengths (painted by grey) and the MOR transmission is close to the transmission of a non-resonator.

In the magnetic field when $\varphi = \pi / 2$ the fringes of constant inclination are clearly visible again. However, their color distribution has changed. In this case the two orders of interference are observed: the truncated blue end first order and the second one when $\theta_1 > 33^0$. Such changes of the angular dispersion are caused by the inversion of the interference extrema in polychromatic light.

3.2 Experimental results

For the measurements of spectra, the free plane-parallel plates of *n*-InAs were used as a simple Fabry-Perot resonator. The high value of the refraction factor $n \approx 3$ caused a value of the reflection coefficients of the faces - mirrors $\rho_1 = \rho_2 \approx 0.25$.

Semiconductor *n*-InAs is isotropic in the absence of a magnetic field. The high concentration of the free electrons $N_q = (1.3 \div 1.4) \cdot 10^{18}$ cm^{-3} made possible to carry out the measurements in a classical magnetic field: the Landau splitting energy is assumed to be small as compared to the thermal electron energy.

The plates were cut from a single crystal bar, then ground and subsequently polished on the broad faces. The 10×10 mm^2 samples had thickness $d = 80$ and 100 μ m; the deviation from plane-parallelism was no greater than a few seconds of arc.

The plate was placed between the magnet poles so that the magnetic field was directed normally to the broad faces of the sample. The measurements of spectra were carried out by Fourier-spectrometer (FTIR) with a resolution of 2 cm^{-1}, the aperture of the inlet of the optical equipment did not exceed 2.5^0. The experimental setups for investigating spectra of transmission and thermal radiation are shown in Fig. 6 and Fig. 7.

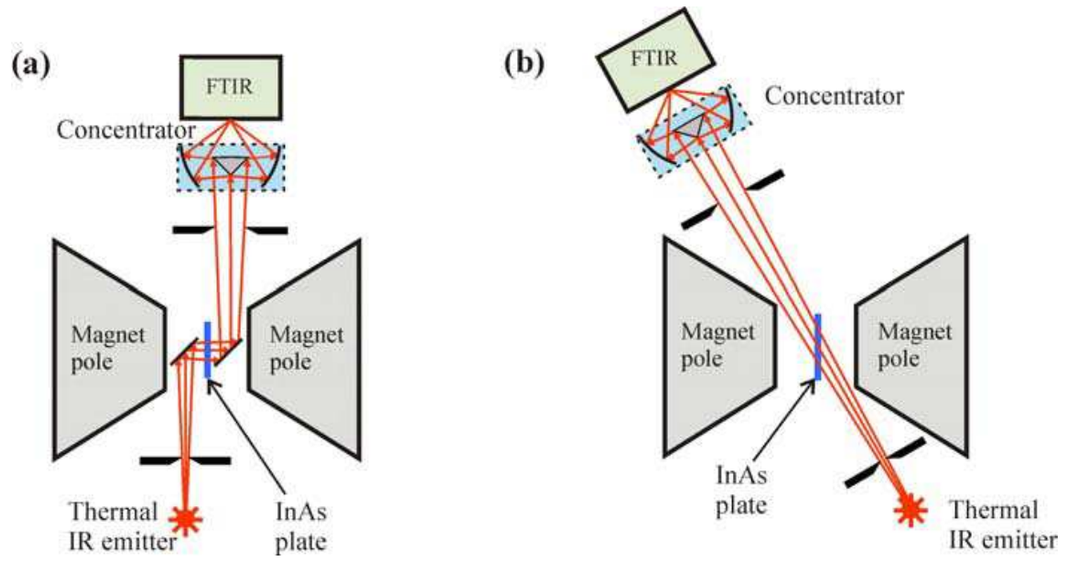

Fig. 6. Experimental setups for investigating transmission spectra of a plane-parallel n-InAs plate in a magnetic field at normal (a) and oblique incidence (b) of unpolarized light.

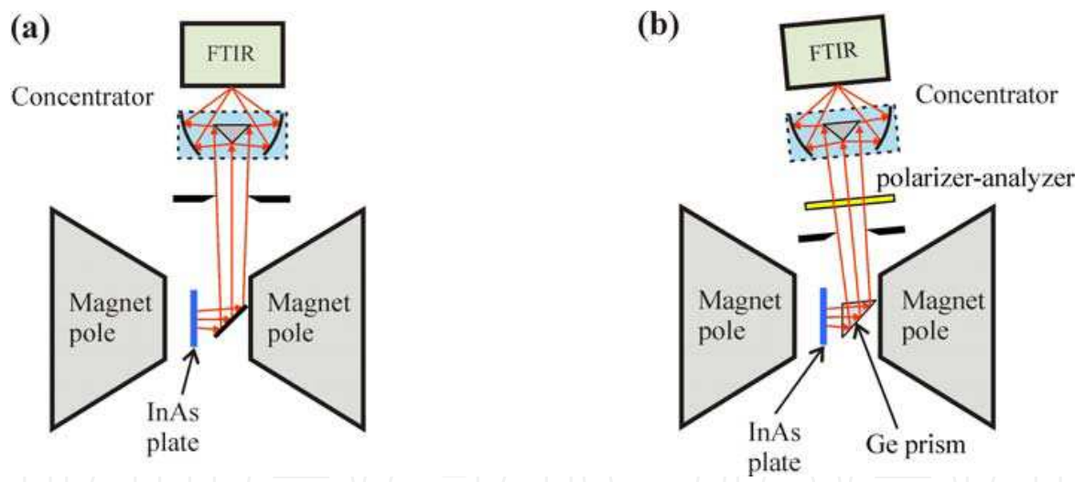

Fig. 7. Experimental setups for investigating spectra of thermal radiation of a plane-parallel n-InAs plate in a magnetic field: (a) - for investigating the total thermal radiation spectra; (b) - for analysis of the circular polarized modes of thermal radiation.

3.2.1 Transmission spectra

Fig. 8 shows the spectral dependencies of transmission of the plate at normal incidence in the absence of the magnetic field (blue line) and in the magnetic field (red line). As it is seen, the dependence $T(\lambda)$ at $H = 0$ has an oscillating form, that is typical for the Fabry-Perot resonator. Positions of the maxima and minima can be estimated from the interference conditions $\lambda_{\max} k = 2n(\lambda)d$ and $\lambda_{\min}(2k+1) = 4n(\lambda)d$ respectively ($k = 1,2,3...$). Unfortunately, the semiconductor n-InAs has a strong dispersion of the absorption

coefficient: $\alpha \propto \lambda^3$ (Madelung, 2004). For this reason contrast of the interference pattern decreases when λ increases.

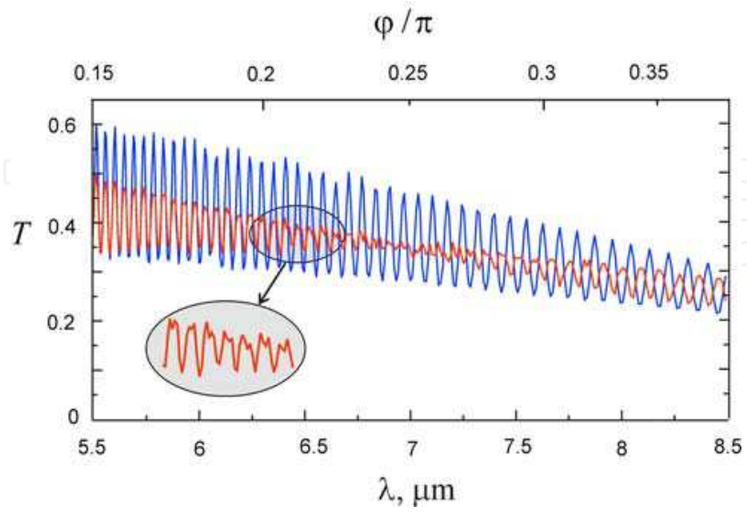

Fig. 8. Experimental transmission spectra of the free plane-parallel *n*-InAs plate at a normal incidence of unpolarized light. $d = 100$ μ m. Blue line: $H = 0$; red line: $H = 24$ kG

In the magnetic field the oscillating spectrum transformed into an oscillating spectrum with a link. A splitting of the maximums into two secondary ones is clearly visible in the spectral range $6.5 < \lambda < 7.3$ μ m. In the range $7.3 < \lambda < 7.6$ μ m (the link range) the secondary maxima are equidistant. Since their amplitudes are less than the zero-field ones, this is revealed as the doubled quantity of illegible interference maxima in the spectrum.

With a further increasing λ ($7.6 < \lambda$ μ m) the secondary maxima merge and the contrast grows. However, the phase of the interference extrema is inverted relative to the $H = 0$ case.

Let us regard this effect from the point of view of Faraday rotation. Since the value of φ depends on wavelength, the analysis of the spectral dependence makes possible to analyze the changes of the interference pattern in the dependence on the value of Faraday rotation at the constant magnetic field. The value of φ, that is shown on the upper scale, was calculated according to the expression:

$$\varphi = \pi \frac{d}{\lambda} \sqrt{\varepsilon_\infty} \left(\left(1 - \frac{\lambda^2 / \lambda_p^2}{(1 + \lambda / \lambda_c)} \right)^{1/2} - \left(1 - \frac{\lambda^2 / \lambda_p^2}{(1 - \lambda / \lambda_c)} \right)^{1/2} \right), \tag{10}$$

where $\lambda_c = 2\pi m^* c^2 / qH$ is a wavelength of the cyclotron oscillations, $\lambda_p = c\sqrt{\varepsilon_\infty m^*} \Big/ q\sqrt{N_q}$ is a wavelength of the plasma oscillations, q is the electron charge, ε_∞ is the RF permittivity, m^* is an electron effective mass, c is the velocity of light.

The waves j'_ξ (see Fig.2) coming out at $\theta_1 = 0$ remain unpolarized. However the planes of polarization of their components are rotated at 2φ relatively to the corresponding components of the wave $j'_{\xi-1}$ (for example, the marked component E'_1 are rotated relatively

to the E_0' on Fig.2). It leads to the violation of the conditions of interference between them. The result of their superposition is, in general, an elliptically polarized wave. And as a result, the contrast of an interference pattern decreases.

When $\varphi = \pi / 4$ the planes of polarization of the components are rotated at $2\varphi = \pi / 2$, i.e. are orthogonally related. The result of their interaction is not intensification or attenuation, but, in general, an elliptically polarized wave. In this area of wavelengths there is a link in the spectrum of T. The difference of the contrast from zero at $\lambda \approx 7.5$ μm is explained by interference of waves j'_{ξ}, $j'_{\xi+2}$, $j'_{\xi+4}$ … . Their electrical fields are parallel but differ greatly in amplitudes.

At a further increasing λ the angle 2φ exceeds the value $\pi / 2$. It results in appearance of interference extrema. At $2\varphi = \pi$ the electrical fields of the coherent components become parallel again, however their phase difference is $2\delta + \pi$ where $\delta = 2\pi nd / \lambda$ is a phase difference when $H = 0$. It is a reason of the inversion of interference extrema.

With a normal incidence of light the transmission of resonator in a magnetic field can be described by the sufficiently compact analytical expression, which is obtained from Eq. (6):

$$T = \frac{1}{2} \cdot (1 - \rho_1)(1 - \rho_2)\eta \left(\frac{1}{Z(\delta_c)} + \frac{1}{Z(\delta_e)} \right) = T_c + T_e \,. \tag{11}$$

Here $Z(\delta_{c,e}) = 1 - 2\eta\sqrt{\rho_1\rho_2}\cos(2\delta_{c,e}) + \eta^2\rho_1\rho_2$, $\delta_c = \delta + \varphi$, $\delta_e = \delta - \varphi$.

As it is seen, transmission spectrum is the sum of two independent terms, which describe "compressed" (T_c) and "extended" (T_e) spectrum with the increased (δ_c) and reduced (δ_e) on φ phase difference respectively. Since these spectra have different interference fringe spacing, depending on the relationship δ_c and δ_e they can be in phase, antiphase or in-between state. They can also be in the same state relative to the zero-field spectrum. The diverging of the maxima T_c and T_e is observed in the complete transmission spectrum as a splitting of the interference maxima. One secondary maximum corresponds to T_c and the other one corresponds to T_e.

When these spectra are in antiphase, they substantially compensate each other. In this region the link is observed. With a further increasing φ the maxima T_c and T_e begin to approach and merge, being, however, in antiphase to the original spectrum. The inversion of interference extrema is observed here.

Note that similar processes determine behavior of the discussed above angular dependences. However, for oblique incidence the reflection of real mirrors depend on the angle of incidence. In this case, they are also polarizing elements. This fact complicates the description of the process, though its essence remains the same.

Fig. 9 presents the experimental transmission spectra of the plate at angle of incidence $\theta_1 = (70 \pm 1)^0$. Note two features of this spectrum. First, in this case the link is located in the region $\varphi \approx 0.18\pi$. Second, there is a sagging of the transmission spectrum in the field relative to the zero-field spectrum.

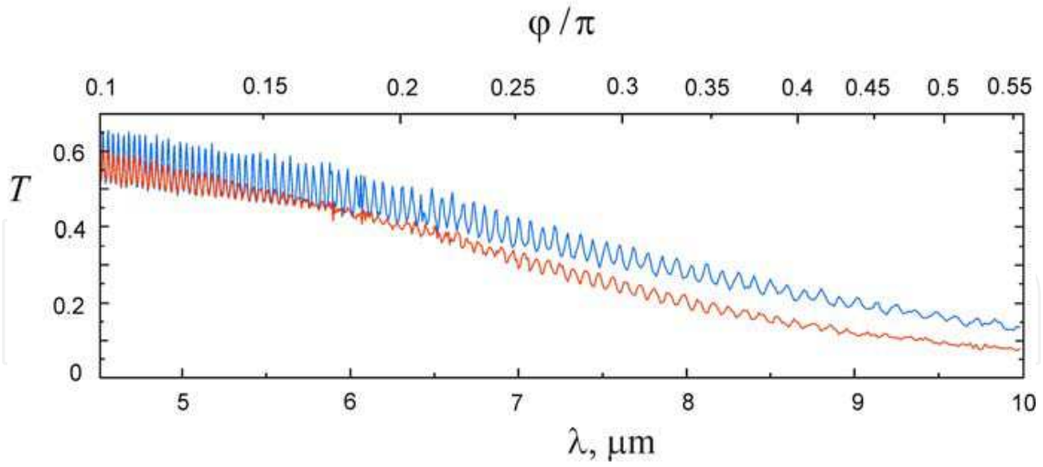

Fig. 9. Experimental transmission spectra of the free plane-parallel *n*-InAs plate at an angle of incidence $\theta_1 = (70 \pm 1)^0$. Light is unpolarized. Blue line: $H = 0$; red line: $H = 24$ kG

These features are caused by the polarizing action of the plate faces, whose reflection becomes anisotropic at oblique incidence: reflection of s- polarized component predominates above the reflection of the p- polarized one. For this reason the entered to the resonator light is partially polarized with the predominance of p- polarization. Faraday rotation leads to redistribution of the polarization of waves. With the approach the opposite face the light radically differs in degree and type of polarization from that entered. Interaction of light with the constantly changing polarization characteristics with the anisotropic mirrors leads to features of both the interference pattern and the absolute values of the resonator transmission.

Though the sagging of the spectral dependence T is not related to the interference effects, this fact is sufficiently interesting. Let us consider this fact in detail. For this, after excluding reflection for p-polarized light and interference, from Eq. (6) one can obtain the dependence of the transmission of a nonresonant magneto-optical sample on φ at the angle of incidence, equal to the Brewster angle ($\theta_1 = \theta_B$):

$$T^* = \eta \frac{2(1-\rho) + \rho^2 \cos^2(\varphi)\left(1 - \eta^2 \cos(2\varphi)\right)}{2\left(1 - \eta^2 \rho^2 \cos^4(\varphi)\right)}, \tag{12}$$

where $\rho = (n\cos(\theta) - \cos(\theta_1))^2 / (n\cos(\theta) + \cos(\theta_1))^2$.

Note that the angle of incidence 70^0, which was used in the experiment, is very close to the Brewster angle. As it is seen from Eq. (12), the value of the transmission of unpolarized light at $\theta_1 = \theta_B$ is a function of the single-trip Faraday rotation angle. This does not lead to violation of the energy conservation law, since the decrease of energy of transmitted light is compensated by an increase of the energy of reflected and absorbed light.

Thus, the Faraday rotation not only changes the conditions of interference, but also redistributes an energy between the transmitted and reflected light.

3.2.2 Spectra of thermal radiation

Fig. 10 presents the measured spectra of TR of the plate in the absence of the magnetic field (blue line) and in the magnetic field. The experimental setup for this investigation is shown in Fig. 7a. Behavior of the TR spectrum is qualitatively similar to the behavior of the transmission spectrum. Here it is also observed the splitting of maxima into two secondary ones, which pass into the link.

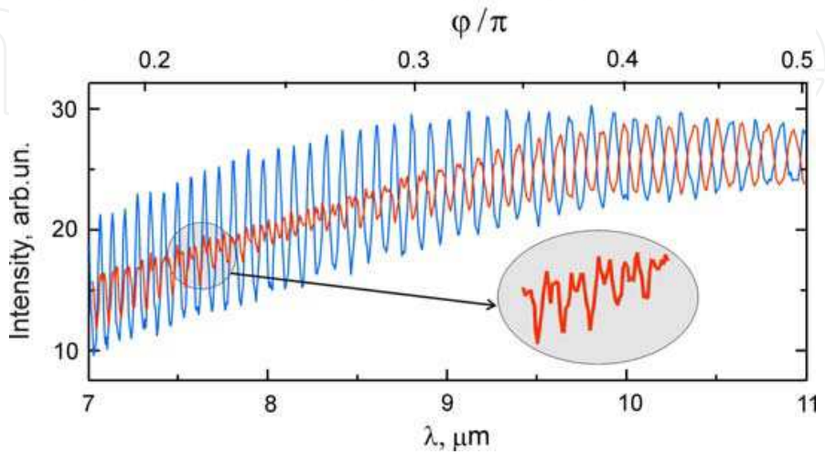

Fig. 10. Experimental spectra of thermal radiation of a free plane-parallel n-InAs plate at normal incidence, $d = 100$ μ m. Blue: $H = 0$; red: $H = 18$ kG; temperature is 355 K.

With a further increasing λ and, respectively φ, the secondary maxima begin to merge, forming clear interference pattern. In this case the inversion of interference extrema occurs too.

As for T, it is possible from Eq. (9) to obtain an analytical expression for the emissivity of MOR from a mirror ρ_1 at the normal incidence:

$$A = \frac{1}{2}\cdot(1-\rho_1)(1+\eta\rho_2)(1-\eta)\left(\frac{1}{Z(\delta_c)}+\frac{1}{Z(\delta_e)}\right). \tag{13}$$

It is seen that TR also consists of two independent modes with different spectral dependences. Taking into account that the value of the single-trip Faraday rotation angle is:

$$\varphi = \frac{\pi}{\lambda}d\left(n_+ - n_-\right), \tag{14}$$

where $n_\pm$ are refractive indexes of a right-hand and a left-hand circular polarized light, for the linear approximation $n = (n_+ + n_-)/2$ Eq. (13) can be converted to the form:

$$A = \frac{1}{2}\cdot(1-\rho_1)(1+\eta\rho_2)(1-\eta)\left(\frac{1}{Z(\delta_+)}+\frac{1}{Z(\delta_-)}\right). \tag{15}$$

Here $\delta_\pm = 2\pi n_\pm d/\lambda$. It becomes obvious that the TR modes are right-hand and a left-hand circular polarized. Using this fact, we can experimentally separate them and measure separately.

For separation and analysis of circular polarized light a germanium total internal reflection prism with base angles of $43°$ was used. Its principle of operation is analogous to that of Fresnel prism: it brings about a phase difference of $\pi/2$ between the perpendicular components of radiation. Since the polarization planes of right- and left-hand polarized radiation are mutually perpendicular, the required radiation modes was separated by applying a polarizer-analyzer and recorded by the FTIR. Besides, the prism served as a deflecting element to take the sample radiation out of the gap between the magnet poles (see Fig.7b).

Fig. 11 shows the spectra of the right- and left-hand circular polarized modes of TR, respectively. One can see easily that the oscillation phases of these spectral patterns do not coincide. The oscillation phase of the right-hand circular polarized mode takes the lead over that of the left-hand circular polarized mode, and at $\lambda \approx 9.2$ μ m they are in antiphase.

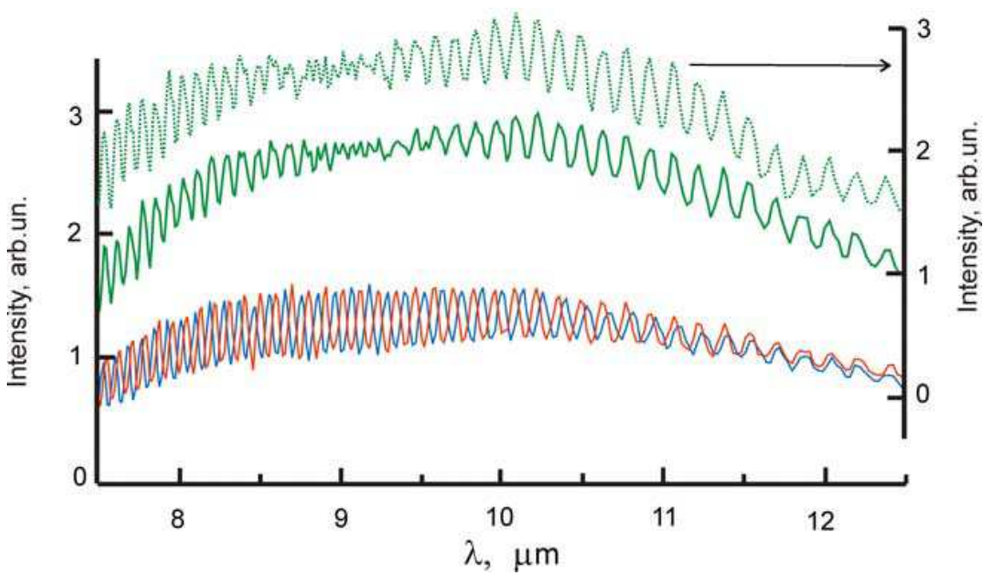

Fig. 11. Experimental spectra of thermal radiation of a free plane-parallel n-InAs plate in the magnetic field $H = 15$ kG. $d = 100$ μ m. Red and blue lines are a right-hand and a left-hand circular polarized mode respectively; green line is a sum of the modes; green dot line is a total TR spectrum (a right axis). Temperature is 375K.

The solid green line is an arithmetical sum of the right-hand and left-hand circular polarized modes spectra; it agrees well with the total TR spectrum recorded without a polarizer-analyzer (the dot green line). Some insignificant distinction between amplitudes of this spectrum is due to the losses introduced by the polarizer-analyzer.

4. Applications

4.1 Determination of parameters of solids

The experimental investigations of the optical properties of solids make possible to obtain the extensive information about their physical properties and parameters. Among the

magneto-optic methods of the investigations the Faraday effect is in highlight. It makes it possible to determine, for example, the effective mass of free carriers in the semiconductors, its temperature and concentration dependences and thus to conclude about the form of energy bands.

The applied methods of determination the magnitude of the Faraday effect consist in the measurement of intensity of linearly polarized light that is transmitted through the sample and polarizer-analyzer. The changes of intensity, which appear in a magnetic field, are compensated by the turning of polarizer-analyzer or are measured by a register.

Since the measurements have an absolute nature, an error in the measurement of rotation angle is determined by error in the determination of a light intensity change and an intensity of light itself. Besides the random errors of measurements the systematic errors can arise, that is caused by the imperfection of the used polarization devices, the inhomogeneity of the samples and their surfaces, the multiple reflection of light in thin crystals and others. The last forces researchers to guard, for example, to make the samples in the wedge form.

According to the results of investigations given above the multibeam interference is not the parasitic effect, which puzzles the researchers of the Faraday effect. Moreover, the presence of interference together with the Faraday rotation makes possible to determine the magnitude of the Faraday rotation angle rapidly and reliably using affordable equipment.

It is simple to obtain from Eq. (11) and Eq. (12) the envelope functions (that determine the dependence on λ of the oscillation maxima and minima, respectively) for the oscillating functions of transmission ($T^{(-)}$, $T^{(+)}$) and emissivity ($A^{(-)}$, $A^{(+)}$). They have the following form:

$$T^{(\pm)} = \frac{(1-\rho_1)(1-\rho_2)\eta}{1 \pm 2\eta\sqrt{\rho_1\rho_2}\cos(2\varphi) + \eta^2\rho_1\rho_2} \tag{16}$$

$$A^{(\pm)} = \frac{(1-\rho_1)(1+\eta\rho_2)(1-\eta)}{1 \pm 2\eta\sqrt{\rho_1\rho_2}\cos(2\varphi) + \eta^2\rho_1\rho_2} \tag{17}$$

Applying the same transformation to the Eq. (7) it can be obtained analogous envelope functions for the reflection:

$$R^{(\pm)} = \frac{\left(\rho_1 \pm 2\eta\sqrt{\rho_1\rho_2}\cos(2\varphi) + \eta^2\rho_2\right)}{1 \pm 2\eta\sqrt{\rho_1\rho_2}\cos(2\varphi) + \eta^2\rho_1\rho_2} \tag{18}$$

Solving the equations $T^{(-)} = T^{(+)}$, $A^{(-)} = A^{(+)}$ and $R^{(-)} = R^{(+)}$ it is easy to determine that the envelope functions cross at a point $\varphi = \pi/4$. This result confirms above empirical conclusion that the link position corresponds to the Faraday rotation angle $\varphi = \pi/4$. This is a convincing base for use a registration of the spectral dependence T, either R or TR for the determination of the value of Faraday rotation from the position of link.

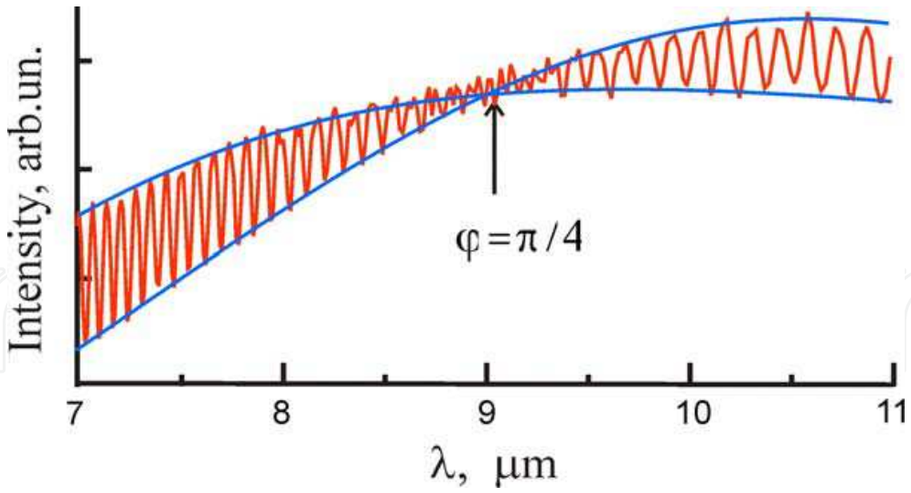

Fig. 12. Experimental spectra of thermal radiation of a free plane-parallel n-InAs plate and envelope lines (blue lines), $d = 80$ μm. $H = 18$ kG; temperature is 355K.

Fig.12 shows the experimental spectra of TR of the free plane-parallel n-InAs plate and envelope lines (blue lines). The link has a certain extent in the spectrum. Determination its position "by sight", causes a certain error. This error is insignificant. In this case the determined "by sight" spectral extent of the link is approximately $8.9 - 9.25$ μ m, which introduces error into the determination of the Faraday rotation angle $\varphi = 45^0 \pm 1.7^0$ deg. The determined according to the point of intersection of the envelopes functions spectral position of the value $\varphi = \pi / 4$ is equal to 9.07 μ m.

The accuracy of the determination of semiconductor parameters from the value φ depends also on the accuracy of the determination of the resonator thickness d and its refractive index n. The d value is determined by technological process and can be known with the high accuracy but n can greatly changes depending on the type and level of doping, as well as on the wavelength. And in this case the presence of interference becomes very useful factor again. As it is known, the interference fringe spacing is determined by the factor nd / λ. Knowing precise value d it is possible to determine n very accurately by analyzing the spectral characteristic without magnetic field. For the used in the experiment sample $n = 3.08$ in the range $\lambda = 8.9 - 9.2$ μ m.

Using the experimental data, the effective mass of electrons in applied semiconductor n-InAs at a temperature of 355 K was determined by the described method. Its value $m^* / m_q = 0.04$ (m_q is the electron mass) matches the reference data (Madelung, 2004).

The advantages of the described method are obvious:

- the measurements can be carried out by using the unpolarized light. This makes it possible to exclude the polarizers and analyzers and thus to simplify both an optical scheme and registering equipment.
- the analysis of spectra without field and in the field makes possible to determine several parameters of the material at once: refractive index and its dispersion, the thickness of magneto-optical layer, the value of φ.

- caring out the measurements with several magnitudes of a magnetic field, it is easy to determine the spectral dependence of φ. This makes it possible to determine such important parameters of semiconductor as the frequency of plasma oscillation, the concentration of the free charge carriers and doping impurity.
- the measurements have not absolute, but relative nature. The accuracy of the method is determined exclusively by the accuracy of the determination of magnitude of *H* and by the quality of the record of interference pattern, and it does not depend on the position of base line. This fact is very important. This makes it possible to get rid of many systematic errors, added both by optical background and measuring optical and electronic equipment into the value of *T* or *R* or TR.
- the method makes possible to carry out the investigations successfully when a magneto-optical layer is located on an opaque substrate. In this case φ cannot be determined by the classical scheme of the Faraday effect investigation. However, as it was shown, TR contains all necessary information and can be used successfully. For this purpose it is necessary only to heat the investigated sample to temperature, higher than background.

4.2 Sources of IR radiation

Currently, infrared radiation sources are used extensively in researches, systems of gas analysis, spectroscopy, medicine etc. While in near-infrared ($\lambda < 2\ \mu$ m) the light-emitting diodes (LEDs) are used successfully, in medium-wave (MWIR) and long-wave IR (LWIR) an external quantum efficiency still abruptly reduces.

At present, in these ranges they use cheap and reliable thermal emitting elements (globar, Nernst pin et al.) with modulation of continuous emission by mechanical modulators. The disadvantages of these sources are nonselectivity of emission and the impossibility to create the pulse-periodic structure of output light flux. In addition, they require optical filters or monochromator. This leads to an increase of electric energy demand, growth of weight and dimensions of the device.

However, the use of medium-wave and long-wave ranges of IR spectrum significantly expands the scope of application of optical instruments. It is caused by the following:

- in these ranges there are the atmospheric transparency windows, and thus, the light waves can spread over long distances;
- many substances have characteristic features in these ranges which allows to detect and recognize them with great accuracy;
- the LWIR range encloses the maximum of thermal radiation of objects with temperature 10^0-100^0 C, i.e., of most of ambient objects. It is very important for systems of analysis, control and monitoring.

For creation of the modern systems of IR engineering and optoelectronics it is necessary that the source could work in the pulse or in the pulse-periodic regimes of generation of noncoherent radiation. Also there is a special interest in the sources with smooth tuning of spectral characteristic.

The researchers pin their hopes on the quantum well based LEDs, which construction and composition makes possible to expand the radiation range to $\lambda \approx 8-10$ μ m (Das et al, 2008; Yang et al, 1997) and even to create LED with two color spectral characteristic of emission (Das, 2010). However, the intensity of emission of such devices at room temperatures in LWIR does not exceed several μ W.

The promising concept of the problem solution is to use the non-luminescent (thermal) semiconductor sources as the IR emitters. The control over their TR intensity is exerted via variation of the absorption coefficient beyond the semiconductor fundamental absorption edge by varying the free charge carrier concentration. The physical principles of operation and constructions of some semiconductor TR sources are described, for example, in (Malyutenko, Bolgov et al., 2006). The advantage of the IR sources is that they do not require additional modulation facilities. However, they have a broad ($\lambda \approx 2-18$ μ m) spectrum of radiation. Therefore the additional filters are needed when narrow-band radiation is required.

New potentialities in realization of controllable narrow-band thermal sources of IR radiation appear when structures with coherent TR are used as a radiation elements. Recently, there are two different approaches to achieve the coherent thermal radiation, highly directional in a narrow spectral range. The first one is to use the materials in which there are the surface-phonon (plasmon) polariton waves: polar dielectrics, doped semiconductors or metals (Biener et al., 2008; Celanovic et al., 2005; Greffet et al., 2007; Lee et al., 2008). Since surface waves decay exponentially from the interface, the conversion from the evanescent mode to traveling mode is achieved by properly designing a periodical microstructure, for example, grating on an emitting material. Their TR is characterized by a strong peak at a certain frequency typical for the surface polariton excitations. The appropriate control can be provided by varying the material of the radiating structure (phonon mechanism) or the free carrier concentration in the same material (plasmon mechanism).

The second approach is to use semitransparent plane-parallel mono- or multilayer resonator structures (Drevillon et al., 2011; Jérémie & Ben-Abdallah; 2007, Kollyukh et al., 2003; Laroche et al., 2006; Lee & Zhang, 2007; Morozhenko & Kollyukh, 2009). Such resonators are very applicable for development of the controllable narrow-band IR sources. TR from the resonators occurs for both polarizations. It makes it possible to increase an intensity of radiation.

Application of the magneto-optical materials enables to change dynamically the optical characteristics of resonator by an external magnetic field and to control parameters of their TR.

Fig. 13 shows the theoretical spectral dependencies of emissivity of a magneto-optical resonator in the different magnetic fields, that is shown in φ units. Since the thickness of resonator is small in comparison with the wavelength, the zero-field spectrum (at $\varphi = 0$) is a number of the narrow widely distant behind each other lines. Their maxima are practically equal to 1, that corresponds to the TR intensity of the blackbody at the same temperature.

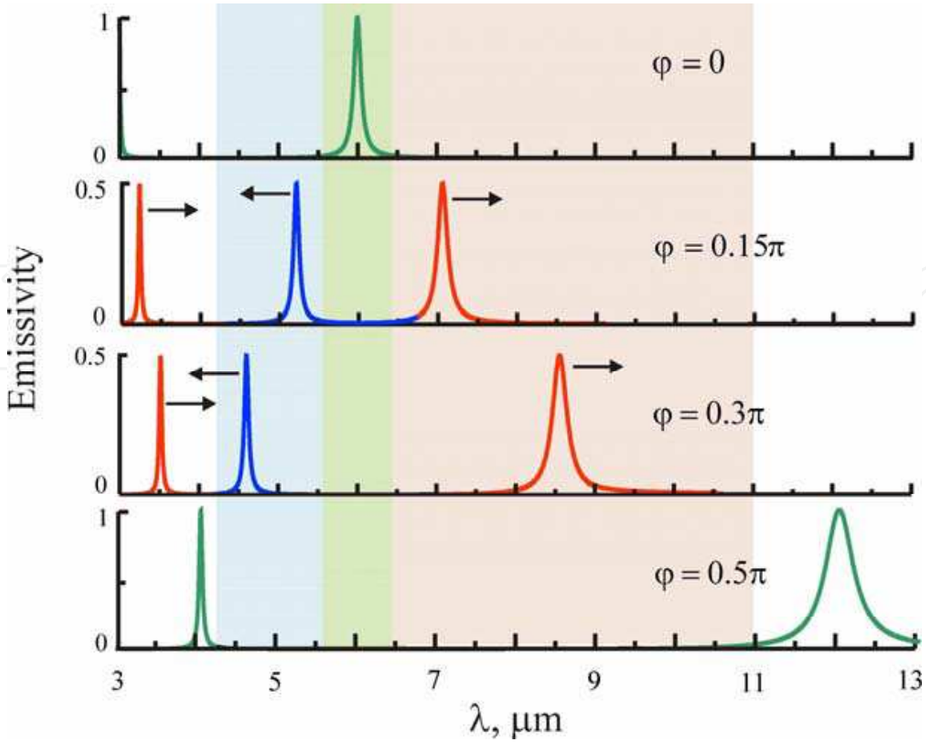

Fig. 13. Calculated emissivity spectra of a magneto-optical Fabry-Perot resonator at normal propagation of TR. $\rho_1 = 0.95$, $\rho_2 = 1$, $d = 1$ μm, $n = 3$, $\alpha = 300$ cm^{-1}.

The line width of the radiation ($\Delta\lambda$) is determined by the parameters of resonator. When the resonator Q factor is high and condition $\varsigma = \eta\sqrt{\rho_1\rho_2} \approx 1$ is satisfied, $\Delta\lambda$ on the half-height of emissivity are described by the expression:

$$\Delta\lambda \approx \frac{\lambda_{\max}(1-\varsigma)}{\pi\sqrt{\varsigma}} \tag{19}$$

Here it is assumed that the dispersion n is disdainfully small in the spectral range of line.

As it is seen on Fig.13, in the magnetic field these lines split into two narrow lines with maxima 1/2, which are diverge into the red and blue range of the spectrum. In the under consideration spectral range it is possible to mark out several characteristic areas: the area "of amplitude modulation" of the emission line, which corresponds the zero-field line (it is shown by green color), and two areas "of control of radiation spectrum" (blue and pink colors). These areas are named in accordance with their possible application for developing of the narrow-band IR source with the controllable characteristics. Let us consider each of them.

4.2.1 Source with the amplitude modulation of intensity

The development of IR sources with the internal modulation of intensity is very urgent for such equipments as, for example, optical IR gas analyzers. In the optical gas analyzers a gas concentration is measured by the magnitude of light absorption in the characteristic

absorption band. The advantage of the gas analyzers in comparison with the other types (electrochemical, thermocatalytic, semiconductor) is caused by the following factors: proximity and nondestructive nature of the measurements; selectivity; quick-action and the ability to carry out measurements in real time; a uniquely wide range of measurement.

To realize all these advantages of optical gas analyzers it is necessary to have a narrow-band light source with radiation maximum that corresponds to the absorption band of the measured gas, and with the possibility of internal modulation of intensity. The last characteristic makes possible to exclude the modulating device from the construction of gas analyzer.

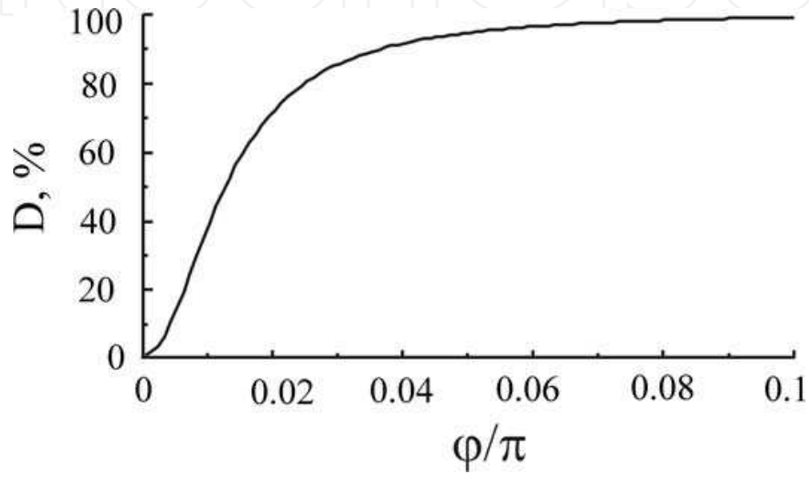

Fig. 14. Dependence of the amplitude modulation index of TR in the spectral range of the zero-field line $5.95 < \lambda < 6.05$ μ m on the single-trip Faraday rotation angle.

This source of MWIR and LWIR radiation can be realized, if the observation is carried out in a spectral range of the zero-field line. By application of a magnetic field the secondary lines of TR leave this range and the intensity of radiation becomes practically zero. The dependence of amplitude modulation index $D = (I_{TR}^0 - I_{TR}^H)/(I_{TR}^0 + I_{TR}^H)$ (here I_{TR}^0 and I_{TR}^H are the intensities of TR at $H = 0$ and $H \neq 0$ respectively) on the Faraday rotation angle in a spectral range of the zero-field line ($5.95 < \lambda < 6.05$ μ m) is shown on Fig. 14. As it is seen, unity modulation of the intensity of the radiation line is reached already at $\varphi \approx \pi / 10$.

In addition, as it can be seen from Fig.11, this source of IR radiation is multicolored, that is very important, for example, for testing multi wavelength IR sensors.

4.2.2 Sources with controllable spectral characteristic

Narrow-band sources with a tunable radiation spectrum are, actually, the integral spectroscopic device, which includes a source and monochromator in one device. Demand on such sources is obvious: the modern technologies make possible to create the compact chips of information processing, super-dense receiving matrices, fibre-optic paths. However, a presence in the spectroscopic devices of a dispersion element (prism, diffraction grating) with a necessary optical base nullifies all attempts of miniaturization and compactness of the devices.

The frequency-controlled lasers partially fill this niche. But their range of smooth tuning is insignificant. Since such lasers have large sizes, significant consumption of electric power and are expensive, they remain the special-purpose instruments and do not solve the problem of developing of the cheap compact spectroscopic device of general-purpose.

Application of the magneto-optical resonator as the radiating element is the promising way of creating of that sort of sources. As it was shown, blue ($4.3 < \lambda < 5.6$) and red ($6.4 < \lambda < 11$) ranges in Fig.13 are the ranges in which a change of the spectral position of a radiation line is realized. In the blue range $\lambda_{\max}$ of a secondary line is shifted to the short-wave side with an increasing magnetic field. For the order of interference k, one gets

$$\lambda_{\max}^{blue} = \frac{nd}{k + \varphi / 2\pi} \tag{20}$$

In the red range, the shift of $\lambda_{\max}$ occurs into the long-wave side:

$$\lambda_{\max}^{red} = \frac{nd}{k - \varphi / 2\pi} \tag{21}$$

Fig. 15 shows the dependences of the spectral position of the TR line on the single-trip Faraday rotation angle for these two regions. The ranges of spectral tuning of emitter are bounded by the edge of an zero-field line from one side and by the edge of line at $\varphi = \pi / 2$.

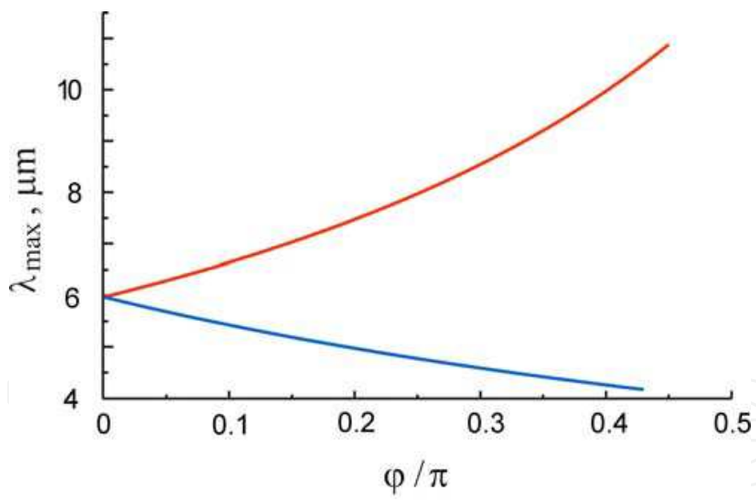

Fig. 15. Dependence of the spectral position of TR lines on the single-trip Faraday rotation angle in the blue (blue line) and red (red line) ranges.

Thus, the range of the radiation spectrum tuning (Λ) of this source is approximately equal to half of the interference fringe spacing at $H = 0$ and depends on the thickness of resonator and order of interference.

Dependences of the blue and red ranges on the thickness of resonator are shown on Fig.16 for the orders of interference 1, 2, and 3. It is seen that for realization of control of the source spectrum in a broad range it is necessary to have the strong Faraday rotation ($\varphi \le \pi / 4$) in

the short optical base equal to several micrometers. In addition, that the resonator could work as a thermal IR source, it is necessary that its temperature exceeds the temperature of background (ambient temperature). This imposes the strict requirements on the magneto-optical medium of resonator.

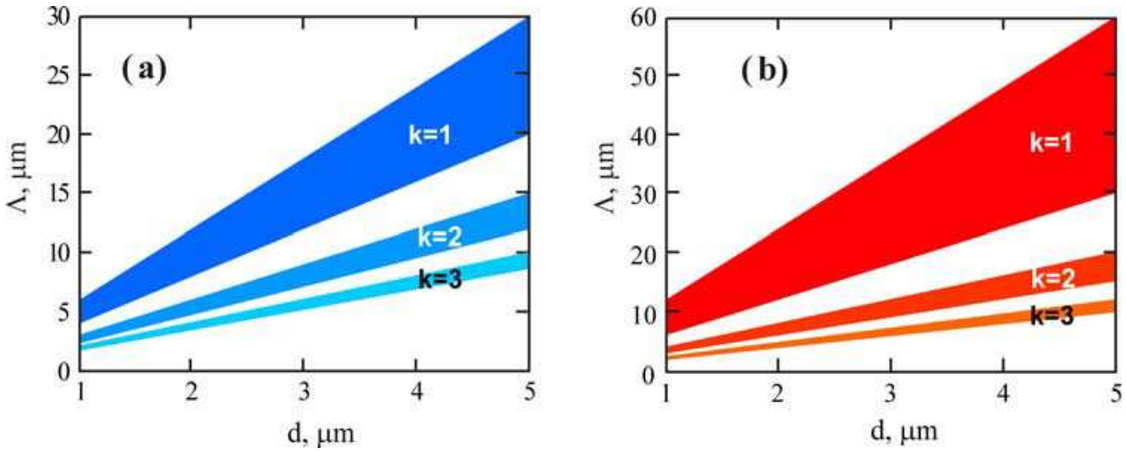

Fig. 16. Dependences of the blue (a) and red (b) ranges on the thickness of resonator for the orders of interference $k = 1, 2$ and 3.

These devices can be applicable in many fields of engineering, science, medicine, technology etc.

4.2.3 Sources with control of spatial field of radiation

At present time the infrared optical-electronic systems, devices of thermal imaging and IR cameras are used in many areas of science and technology. Checking of their functionality, calibration and testing of their characteristics are an important task. Therefore the urgent problem is the development of methods of simulating and creation of the IR sources, spatial coordinates and intensity of radiation of which can dynamically change (imitators of the heated objects) (Williams, 1998).

Multielement radiation sources are used traditionally for this purpose. Now the two-dimensional (2D) devices based on electrically heated pixels have been developed and successfully applied (Pritchard et al., 1997; Robinson et al., 2000). Since the radiating element of these devices is the thermal resistor, they make it possible to create 2D field of radiation in a wide range of infrared spectrum. However, thermal control of radiation intensity of a pixel limits the system performance that does not exceed 100 Hz. In addition, in the thermal sources there is a problem of the thermal isolation between control circuit and radiating elements, and also between the adjacent radiating elements.

More promising are systems with the multielement luminescent radiating elements based on semiconductor laser diodes (Beasley et al., 1997; Cantey et al., 2008). These projectors are capable to generate dynamic infrared scenes in real-time. The ability to simulate high apparent temperatures is the result of luminescent infrared radiance emitted by the diode lasers. An operating spectral range of these projectors is $\lambda = 3 - 5$ μ m, that corresponds to the first atmospheric transparency window.

In (Malyutenko et al., 2001) it was researched an array of IR sources based on a narrow-bandgap semiconductor and operating both on the principle of positive and negative luminescence excitation under conditions of the magnetoconcentration effect. The introduced device is capable of creating both positive and negative radiation contrasts relative to the background emission level.

A disadvantage of the all matrix approaches is the fact that adjacent radiating matrix elements are separated by the spaces, needed for the electrical and thermal isolation. This decreases the brightness of matrix. Furthermore, in the matrix sources there is a task of address control of separate elements.

A whole (not matrix) thermal source with large area (several cm^2) with a possibility of coordinate modulation of its emissivity can be released of these disadvantages. In **(**Malyutenko et al., 2003; Malyutenko, Bogatyrenko et al., 2006) it was proposed to use a translucent plate of wide-gap semiconductor Ge or Si (a screen) as 2d radiation source, and a coordinate modulation of the emissivity to achieve by the intrinsic photoeffect. This heated screen was locally illuminated by light of the visible or near IR ranges. As a result of increasing of free carriers concentration in the places of illumination the authors obtained a local increase of TR in MWIR and LWIR ranges.

In the present paper it is proposed to use as a screen a heated MOR with nonuniform thickness and to modulate its emissivity by an external magnetic field.

Let us consider a resonator with non-parallel mirrors (wedge MOR). Since the condition for interference maximum of TR contains a thickness, the interference fringes of TR appear on a surface, each of which is characterized by condition $d = const$ at fixed wavelength. They are called the fringes of constant thickness. Let the MOR thickness changes in the x direction by a simple linear law $d(x) = d_0 + ax$. In this case the position of the radiating area (x_{TR}) with a wavelength λ in a magnetic field is determined from (20) and (21) by expression:

$$x_{TR} = \left(\frac{k \pm \varphi / 2\pi}{n} \lambda - d_0 \right) \cdot a^{-1} . \tag{22}$$

Sign "+" corresponds a secondary line of TR of the "blue" area and "-" corresponds the "red" area.

The spatial distribution of TR is one or more localized on the MOR surface radiative strips that are perpendicular to the axis x. Their position is determined by both the parameters of resonator and by value of Faraday rotation angle (by a magnetic field strength).

Fig.17. shows the calculated distribution of TR intensity on surface of the wedge MOR resonator at the different values of φ for $\lambda = 10$ μ m. With an increasing magnetic field the radiating strip shifts smoothly in direction of larger thickness. The thickness of resonator is chosen here in such way that the rest of the field remains dark. Since this emitter is not multielement, but it is whole homogenous structure, the movement of the radiating strip is realized not discretely but smoothly.

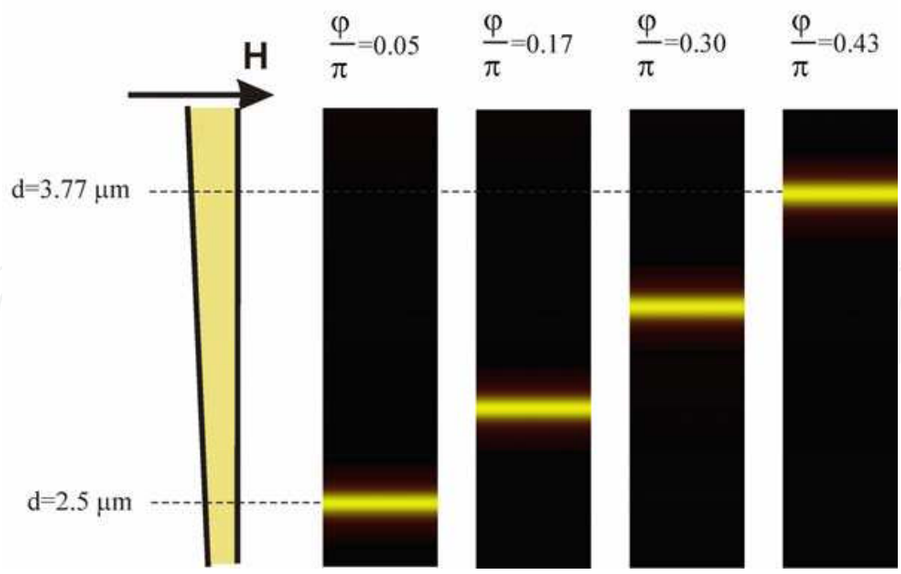

Fig. 17. Calculated fringes of constant thickness of TR of the wedge magneto-optical Fabry-Perot resonator (on the left). $\rho_1 = 0.95$, $\rho_2 = 1$, $n = 3$, $\eta = 0.97$, $\lambda = 10$ μ m, $k = 1$.

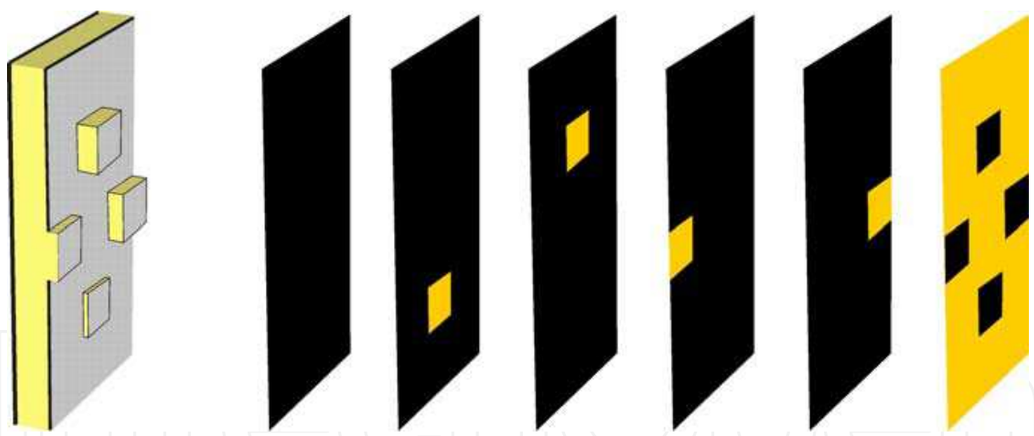

Fig. 18. MOR with the discrete relief on the radiating surface (on the left) and calculated distribution of TR intensity on its surface at the different values φ. $\rho_1 = 0.95$, $\rho_2 = 1$, $n = 3$, $\lambda = 10$ μ m, $k = 1$.

Devices of this type can be used as IR test patterns for calibrating optoelectronic devices with respect to spatial, temperature, and time resolution.

Fig.18 presents the field of TR of MOR with the discrete relief on the radiating surface. Applying the different value of a magnetic field, it is possible to create conditions for the maximum of interference for each of the elements of surface separately, leaving the rest of the surface not radiating. Thus this screen is capable of generating dynamic 2D infrared scenes in real-time by an external magnetic field.

5. Conclusion

In summary, the results of theoretical and experimental investigations of reflection, transmission and thermal radiation of a magneto-optical Fabry-Perot resonator in an external magnetic field are presented. Attention was paid to the investigation of both angular and spectral dependencies of the *T*, *R* and TR in the medium- and long-wave IR ranges for the unpolarized light.

It is established that under the conditions of multibeam interference a magnetic field substantially changes the characteristics of the transmission and reflection of unpolarized light as well as of the own thermal radiation of the resonator. It is shown that the changes also appear for the polychromatic light.

Authors produced a detailed explanation of this effect: the cause of the changes of MOR characteristics is a change of the conditions of the multibeam interference in a magnetic field. A magnetic field redistributes the polarization planes of the light waves inside the resonator. As a result, the interference of the transmitted, reflected and radiated waves can be suppressed or phase shifted by a phase difference of π. The produced in the paper theory is based on the matrix multi-beam summation considering the Faraday rotation effect. The calculation results have a good agreement with experimental data.

In the part "4. Applications" a number of the possible applications of MOR is described. It is shown that the presence of interference in the samples is a favorable factor for investigating the Faraday effect. The determination of the value of the Faraday rotation angle φ by registration the transmission or reflection spectra of unpolarized light or own TR is a convenient way, which has several advantages over the traditional methods. First, it makes it possible to simplify optical scheme and recording system considerably and, thus, to make these studies more available for researchers. Second, since the measurements have relative, but not absolute nature, an error in determining the value of φ is greatly reduced. Third, this way makes possible to determine several parameters of a plane-parallel magneto-optical sample at once. Fourth, analysis of a spectrum of TR makes possible to determine φ in a case, when the classical scheme of the Faraday effect is not applied. For example, when magneto-optical layer is located on the opaque substrate.

Considerable attention is paid to the possibility of creation the controlled IR sources of different purposes with the application of the magneto-optical structures, such as MORs or magnetophotonic crystals. The resonator properties of these objects cause the narrow-band spectrum and the narrow-beam directional diagram of their thermal emission. And the influence of an external magnetic field makes possible to change dynamically the intensity or spectral position of the radiation line, and also to relocate the local radiating regions on the emitter area.

These devices can be applicable in many fields of engineering, science, medicine, criminology, technology etc. The main applications of the IR sources with control of their emission spectrum is the IR spectroscopy and the gas analysis and monitoring of the environment. IR sources with control of spatial field of radiation are very important in order to check the functionality, calibration and testing of their characteristics of the different IR optical-electronic systems. They solve the urgent problem of development of the simulating

methods and creation of the imitators of the heated objects, spatial coordinates and intensity of radiation of which can dynamically change: the dynamic IR scene projectors and scene simulating devices.

For realization of these sources it is necessary to realize the strong Faraday rotation in the short optical base. In addition, it is necessary that emitters' temperature exceeds the temperature of background. This imposes the strict requirements on the magneto-optical medium of the resonator structure. However, authors are assured that the contemporary high technologies are able to synthesize the material, which corresponds these requirements.

In conclusion we have to note, that a magneto-optical Fabry-Perot resonator is a simple case of a magnetophotonic crystal. Further theoretical and experimental investigations of the emitting properties of MPCs in a magnetic field will make possible to determine new peculiarity and effects, which also can be used for the creation of modern optical devices, which can work both with the polarized and unpolarized light in the IR spectral range.

6. References

Beasley, D.B.; Cooper, J.B. & Saylor, D.A. (1997) Calibration and nonuniformity correction of MICOM's diode-laser-based infrared scene projector. *Proc. SPIE.* Vol. 3084. pp. 91-101, ISBN: 9780819424990.

Biener, G.; Dahan, N.; Niv, A.; Kleiner, V. & Hasman, E. (2008). Highly coherent thermal emission obtained by plasmonic bandgap structures. *Appl. Phys. Lett.* Vol. 92, No 8, pp. 081913-1 - 081913-3, ISSN: 0003-6951.

Cantey, T. M.; Ballard, G. & Gregory, D. A. (2008) Application of type II W-quantum-well diode lasers for high-dynamic-temperature-range infrared scene projection. *Opt. Engin.* Vol. 47, Issue 8 pp. 086401, ISSN: 0091-3286.

Celanovic, I.; Perreault, D. & Kassakian, J. (2005). Resonant-cavity enhanced thermal emission *Phys. Rev. B,* Vol. 72, pp.075127-1-6, ISSN: 0163-1829.

Das, N. C. (2010). Infrared light emitting device with two color emission. *Solid State Electron*. Vol. 54, Issue 11, pp. 1381-1383, ISSN: 0038-1101.

Das, N. C.; Bradshaw, J.; Towner, F. & Leavitt, R. (2008) Long-wave (10 micron) infrared light emitting diode device performance. *Solid State Electron*.; Vol. 52, Issue 11, pp 1821-1824, ISSN: 0038-1101.

Dokukin, M. E.; Baryshev, A. V.; Khanikaev, A. B. & Inoue, M. (2009). Reverse and enhanced magneto-optics of opal-garnet heterostructures. *Opt. Express*, Vol. 17, No 11, pp. 9062-9070, SSN: 1094-4087.

Drevillon, J.; Joulain, K.; Ben-Abdallah, Ph.; & Nefzaoui, E. (2011). Far field coherent thermal emission from a bilayer structure, *J. Appl. Phys.* Vol. 109, pp. 034315-1 - 034315-7, ISSN: 0003-6951.

Fujikawa, R.; Baryshev, A.V.; Khanikaev, A.B.; Kim, J.; Uchida, H.; Inoue, M. & Mater. J. (2009). Enhancement of Faraday rotation in 3D/Bi:YIG/1D photonic heterostructures. *J. Mater. Sci. Mater. Electron*. Vol. 20, No. 1, pp. 493-497 , ISSN: 0022-2461.

Goto, T.; Baryshev, A. V.; Inoue, M.; Dorofeenko, A. V.; Merzlikin, A. M.; Vinogradov, A. P.; Lisyansky, A. A. & Granovsky, A. B. (2009a). Tailoring surfaces of one-dimensional magnetophotonic crystals: Optical Tamm state and Faraday rotation. *Phys. Rev. B,* Vol. 79, Issue 12, pp. 125103 - 125103-5, ISSN 1098-0121.

Goto, T.; Baryshev, A. V.; Inoue, M.; Dorofeenko, A. V.; Merzlikin, A. M.; Vinogradov, A. P.; Lisyansky, A. A. & Granovsky, A. B. (2009b). One-way electromagnetic Tamm states in magnetophotonic structures. *Appl. Phys. Lett*. Vol. 95, Issue 1, pp. 011101 011101-3, ISSN 0003-6951.

Greffet, J.J.; Laroche, M. & Marquier, F. (2007). *Microstructured Radiators Final Report.* Ecole Centrale, ASIN: B00383OLFQ, Paris.

Guga, K.Yu.; Kollyukh, O.G.; Liptuga, A. I.; Morozhenko, V. & Pipa, V.I. (2004) Features of thermal radiation of plane-parallel semiconductor wafers. *Semiconductors*, Vol. 38, No 5, pp. 507-511, ISSN: 1063-7826.

Inoue, M. & Fujii, T. (1997). A theoretical analysis of magneto-optical Faraday effect of YIG films with random multilayer structures. *J.Appl. Phys.*, vol.81, No. 8, pp. 5659–5661, ISSN: 0021-8979.

Jacob D., Vallet M., Bretenaker F., Le Floch A., & Le Naur R. (1995). Small Faraday rotation measurement with a Fabry–Perot cavity. *Appl. Phys. Lett.* Vol. 66, Issue 26, pp. 3546-3548, ISSN: 0003-6951.

Jérémie, D. & Ben-Abdallah, P.; (2007) Ab initio design of coherent thermal sources. *J. Appl. Phys.* Vol. 02, Issue: 11, pp.114305-12, ISSN: 0021-8979.

Kollyukh, O.G.; Liptuga, A.I.; Morozhenko, V. & Pipa, V.I. (2005). Magnetic-field modulation of the spectrum of coherent thermal radiation of semiconductor layers. *Phys. Rev.B.* Vol. 71, Issue 7, pp. 073306 - 073306-4, ISSN 1098-0121.

Kollyukh, O.G.; Liptuga, A. I.; Morozhenko, V. & Pipa, V.I. (2003) Thermal radiation of plane-parallel semitransparent layers. *Opt. Commun.* Vol. 225, pp.349-352, ISSN: 0030-4018.

Lancaster, P. & Tismenetsky, M. (1985) *The theory of matrices* (2nd ed.) Academic Press, ISBN: 0-12-435560-9, Orlando, FL.

Laroche, M.; Carminati, R. & Greffet, J.-J. (2006) Coherent Thermal Antenna Using a Photonic Crystal Slab. *Phys.Rev. Lett.*, Vol. 96, No 12, pp. 123903-1 - 123903-3, ISSN: 0031-9007.

Lee, B. J. & Zhang, Z. M. (2007). Coherent Thermal Emission From Modified Periodic Multilayer Structures, *J. of Heat Transfer*, Vol. 129, No 1, pp. 14-26, ISSN: 0022-1481.

Lee, B. J.; Wang, L. P. & Zhang, Z. M. (2008). Coherent thermal emission by excitation of magnetic polaritons between periodic strips and a metallic film, *Opt. Express*, Vol. 16, Issue 15, pp. 11328-11336, ISSN: 1094-4087.

Ling, H.Y. (1994). Theoretical investigation of transmission through a Faraday-active Fabry-Perot etalon. *J. Opt. Soc. Am. A*, Vol.11, No 2, pp. 754-758, ISSN 1084-7529.

Madelung, O. (2004). *Semiconductors: Data Handbook* (3rd ed.), Springer Verlag, ISBN: 978-3-540-40488-0, Berlin.

Malyutenko, V. K.; Bogatyrenko, V. V.; Malyutenko, O. Yu. & Chyrchyk, S. V. (2006). Cold background infrared scene simulation device. *Proc. SPIE*. Vol. 6208, pp. 240-248, ISBN: 9780819462640.

Malyutenko, V.K.; Bolgov, S. S. & Malyutenko, O.Yu. (2001). Multielement IR Sources with Alternating Contrast. *Technical Phys. Lett.*, Vol. 27, No. 8, pp. 644–646, ISSN: 1063-7850.

Malyutenko, V. K.; Bolgov, S. S. & Malyutenko, O. Yu. (2006). Above-room-temperature 3-12 μ m Si emitting arrays. *Appl. Phys. Let.*, vol. 88, pp. 211113-1 - 211113-3, ISSN 0003-6951.

Malyutenko, V.K.; Michailovskaya, K.V.; Malyutenko, O.Yu.; Bogatyrenko, V.V. & Snyder, D.R. (2003) Infrared dynamic scene simulating device based on light down-conversion. *IEE Proc. Optoelectron.*, Vol. 150, No. 4, pp. 391 - 394, ISSN: 1350-2433.

Morozhenko, V. and Kollyukh, O.G. (2009). Angular and spectral peculiarities of coherent thermal radiation of the magneto-optical Fabry-Perot resonator in magnetic field. *J. Opt. A,* Vol. 11, No. 8, pp. 085503-1 - 085503-6, ISSN 1464-4258.

Piller, H. (1966). Effect of internal reflection on optical Faraday rotation. *J. Appl. Phys.*, Vol. 27, No 2, pp. 763-768. ISSN 0003-6951

Pritchard, A.P., Lake, S.P., Balmond, M.D., Gough, D.W., Venables, M.A., Sturland, I.M., Crisp, G. & Watkin, S.C. (1997). Current status of the British Aerospace resistor array IR scene projector technology, *Proc. SPIE,* Vol. 3084, pp. 71-77, ISBN: 9780819424990.

Rheinhlander, B.; Neumann, H. & Gropp M. (1975). Electron effective masses in direct-gap $Al_xGe_{1-x}As$ epitaxial layers from Faraday rotation measurements. *Exp. Techn. Phys.*, Vol. 23, No 1, pp. 33-39, ISSN: 0948-2148

Robinson, R.; Oleson, J.; Rubin, L. & McHugh, S. (2000). MIRAGE: System overview and status. *Proc. SPIE.* Vol. 4027, pp. 387-398, ISBN: 9780819436535.

Rosenberg, R.; Rubinstein, C.B. & Herriott, D.R. (1964). Resonant optical Faraday rotation. *Appl. Optics*, Vol. 3, No 9, pp.1079-1083. ISSN: 0003-6935.

Srivastava, G. P.; Mathur, P. C.; Kataria, N. D. & Shyam, R. (1975). High-frequency effective mass of charge carriers in CdS. *J. Phys. D: Appl. Phys.* Vol. 8, No 5, pp. 523-529.

Stramska, H.; Bachan, Z.; Bysiemki, P. & Kołsodziejczak, J. (1968). Interband Faraday rotation and ellipticity observed at the absorption edge in silicon. *Phys. Stat. Sol. (b)*. Vol. 27, No 1, pp. k25-k28, ISSN: 0370-1972.

Voigt, W. (1908) *Magneto- und Electro-Optic*. Teubner, Leipzig.

Vorobev, L.E.; Komissarov, V. S. & Stafeev, V. I. (1972). Faraday and Kerr effects of hot electrons in n-type InSb in the infrared (II). *Phys. Stat. Sol. (b),* Vol. 52, No 1, p. 25-37. ISSN: 0370-1972.

Wallenhorst, M.; Niemijller, M.; Dotsch, H.; Hertel, P; Gerhardt, R. & Gather, B. (1995) Enhancement of the nonreciprocal magneto-optic effect of TM modes using iron garnet double layers with opposite Faraday rotation. *J. Appt. Phys.* Vol. 77, No 7, pp. 2902-2905 ISSN: 0021-8979.

Williams, O. M. (1998). Dynamic infrared scene projection: a review. *Infrared Phys. Technol.* Vol. 39, Issue 7, pp. 473-486, ISSN: 1350-4495.

Yang, R.Q.; Lin, C-H; Murry, S.J.; Pei, S.S; Liu, H.C; Buchanan, M. & Dupont, E. (1997) Interband cascade light emitting diodes in the 5–8 μm spectrum region. *Appl Phys Lett*; Vol. 70, Issue 15, pp. 2013-2015, ISSN: 0003-6951.

Yariv, A. & Yen, P. (1984). *Optical waves in crystals.* John Wiley & Sons, ISBN 0471091421, New York.

Zhu, R; Fu, S. & Peng, H. (2011). Far infrared Faraday rotation effect in one-dimensional microcavity type magnetic photonic crystals. *J. Magn. Magn. Mater.* Vol. 323, Issue 1, pp. 145-149. ISSN: 0304-8853.

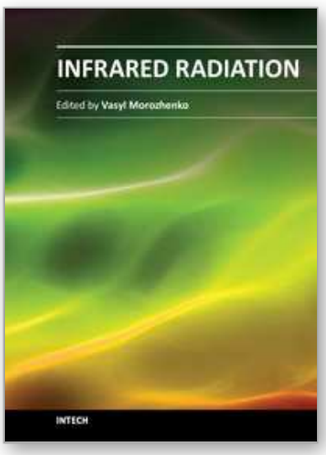

Infrared Radiation

Edited by Dr. Vasyl Morozhenko

ISBN 978-953-51-0060-7
Hard cover, 214 pages
Publisher InTech
Published online 10, February, 2012
Published in print edition February, 2012

This book represents a collection of scientific articles covering the field of infrared radiation. It offers extensive information about current scientific research and engineering developments in this area. Each chapter has been thoroughly revised and each represents significant contribution to the scientific community interested in this matter. Developers of infrared technique, technicians using infrared equipment and scientist that have interest in infrared radiation and its interaction with medium will comprise the main readership as they search for current studies on the use of infrared radiation. Moreover this book can be useful to students and postgraduates with appropriate specialty and also for multifunctional workers.

How to reference

In order to correctly reference this scholarly work, feel free to copy and paste the following:

Anatoliy Liptuga, Vasyl Morozhenko and Victor Pipa (2012). Transmission, Reflection and Thermal Radiation of a Magneto-Optical Fabry-Perot Resonator in Magnetic Field: Investigations and Applications, Infrared Radiation, Dr. Vasyl Morozhenko (Ed.), ISBN: 978-953-51-0060-7, InTech, Available from: http://www.intechopen.com/books/infrared-radiation/transmission-reflection-and-thermal-radiation-of-a-magneto-optical-fabry-perot-resonator-in-magnetic

INTECH
open science | open minds

InTech Europe
University Campus STeP Ri
Slavka Krautzeka 83/A
51000 Rijeka, Croatia
Phone: +385 (51) 770 447
Fax: +385 (51) 686 166
www.intechopen.com

InTech China
Unit 405, Office Block, Hotel Equatorial Shanghai
No.65, Yan An Road (West), Shanghai, 200040, China
中国上海市延安西路65号上海国际贵都大饭店办公楼405单元
Phone: +86-21-62489820
Fax: +86-21-62489821

IntechOpen